

The mechanism model of gas–liquid mass transfer enhancement by fine catalyst particles

Zhang Junmei^{a,b}, Xu Chunjian^{a,*}, Zhou Ming^a

^a The Research Center of Chemical Engineering, School of Chemical Engineering and Technology, Tianjin University, Tianjin 300072, PR China

^b College of Chemical Engineering, Qingdao University of Science & Technology, Qingdao 266042, PR China

Received 21 September 2005; received in revised form 24 March 2006; accepted 27 March 2006

Abstract

In order to present the enhancement of gas–liquid mass transfer by heterogeneous chemical reaction near interface, the mechanism model has been proposed to describe the mass transfer rate for a gas–liquid–solid system containing fine catalyst particles. The composite grid technique has been used to solve the model equations. With this model the effect of particle size, first-order reaction rate constant, distance of particle to gas–liquid interface and residence time of particle near gas–liquid interface on the mass transfer enhancement have been discussed. The particle–particle interaction and slurry apparent viscosity can be considered in the model. The experimental data have been used to verify the model, and the agreement has been found to be satisfied.

© 2006 Elsevier B.V. All rights reserved.

Keywords: Gas–liquid mass transfer; Enhancement; Three-dimensional model; Catalyst particle

1. Introduction

Solid-catalyzed gas–liquid reactions are often encountered in the petrochemical industry, e.g. Fischer-Tropsch synthesis, hydrogenation and oxidation reactions. The transport of component from gas to liquid and to catalyst site frequently limits these reactions rate [1]. It is known that suspended fine solid particles, such as inert particles [2], adsorbents, catalysts or reactants [3], can enhance gas–liquid mass transfer, whereas larger particles showed almost no effect [4].

The enhancement of the specific absorption flux due to the presence of fine particles has been explained by various mechanisms, i.e. boundary layer mixing, shuttling, coalescence inhibition and boundary layer reaction [5]. When small particles catalyze a chemical reaction near gas–liquid interface, significant conversion occurs within the diffusion layer around the gas bubbles, thereby increasing the rate of mass transfer. Mass transfer enhancement during reaction is function of the wettability and activity of the catalyst particles, as well as turbulence intensity in interface.

To study gas absorption into liquid in the presence of fine particles, various mathematical models have been proposed, unsteady-state pseudo-homogeneous models, steady-state heterogeneous models and unsteady-state heterogeneous models. For gas–liquid–solid systems stationary three-dimensional heterogeneous models were developed by Holstvoogd et al. [6] and Karve and Juvekar [7]. In both models a unit cell approach was used, containing single particle in the cell. The models assumed that reaction on particles surface is instantaneous. For gas–liquid–liquid systems, an improved homogeneous model based on film-penetration theory was developed by Nagy and Moser [8], the model accounted for the mass transfer resistance within the dispersed phase and both, first- and zero-order internal and/or external reactions. Unsteady-state, one-dimensional heterogeneous models for one particle in the penetration film considering physical absorption and zero or first-order reaction were proposed by Junker et al. [9] and Nagy [10]. An axisymmetrical two-dimensional heterogeneous mass transfer model based on the general unsteady film-penetration theory considering physical absorption and first-order reaction was developed by Lin et al. [11]. The model assumed the distribution of droplets in continuous phase as a kind of crystal structure, primitive hexagonal cell. Unsteady-state three-dimensional mass transfer model was reported by Brilman et al. [12]. The model has taken into account particle–particle interaction. Homogeneous mod-

* Corresponding author. Tel.: +86 22 27404495; fax: +86 22 27404495.
E-mail addresses: cjxu@tju.edu.cn, cjxu05@eyou.com (X. Chunjian).

Nomenclature

C	concentration (mol/m ³)
C_b	concentration in the bulk continuous phase (mol/m ³)
C^*	concentration at gas–liquid interface (mol/m ³)
C_d	concentration in particle inner surface (mol/m ³)
C_{di}	concentration in particle outer surface (mol/m ³)
D	diffusion coefficient (m ² /s)
d_p	particle diameter (m)
E	enhancement factor
H	Henry's law constant (Pa/mol m ³)
k_1	first-order reaction rate constant in the catalyst surface (1/s)
k_L	liquid side mass transfer coefficient (m/s)
L	distance of particle from the gas–liquid interface (m)
l	distance between particles (m)
N	mass flux of A per unit interface (mol/m ² s)
N^0	mass flux of A per unit interface without dispersed phase (mol/m ² s)
t	Time (s)
<i>Greek letters</i>	
δ	thickness of boundary layer at the gas–liquid interface (m)
ε_s	volumetric holdup of dispersed solid phase
μ	viscosity (N s/m ²)
μ_0	viscosity of continuous (N s/m ²)
μ_{sus}	viscosity of slurry (N s/m ²)
τ_c	gas–liquid contact time (s)

els assumed generally that the dispersed phase droplets are very small with respect to the mass transfer film thickness according to the film theory, mass transfer resistance within the dispersed phase is neglected. Heterogeneous models, taking into account the local geometry at the gas–liquid interface, will increase the level of understanding of the mass transfer enhancement phenomena. In all mathematics model the physical adsorption of particle as major factor was taken into account.

The aim of this work is to develop unsteady-state three-dimensional mass transfer model based on film-penetration theory, which can be used for the case, where the particles size is less than liquid thickness, the mass transfer of sparingly soluble gas is accompanied by first-order chemical reactions on the dispersed catalyst particles surface. The model presents mainly the enhancement of gas–liquid mass transfer by chemical reaction in liquid film.

2. Mass transfer model

2.1. Enhancement mechanism

When the particles are sufficiently small compared to the liquid film thickness, heterogeneous reaction can occur in the

film and the enhancement of gas–liquid mass transfer may be observed. Similar to the ‘shuttle mechanism’, a particle present in the mixed bulk, close to the gas–liquid interface, may move right into the concentration boundary layer. There it adsorbs the dissolved gaseous components and catalyzed chemical reaction, due to their local higher concentrations, the concentration gradient is elevated. Where after the particle may return to the bulk of the liquid, the reactants are desorbed to the bulk slurry until local equilibrium is reached.

2.2. Mathematics model

The relation of mass transfer coefficient k_L and liquid film thickness δ , average surface renewal time τ_c can be represented by

$$\delta = 2\sqrt{\pi D_A \tau_c} \quad (1)$$

In order to simplify mechanism model, the following hypotheses were adopted: (1) the dispersion package in the boundary layer is stagnant during the contact time and the position and distribution of catalyst particles within the package remains unchanged. (2) The gas–liquid interface can be regarded as a plane in a flat interface stirred cell or slurry bubble column reactor where bubbles are large with respect to the particle. (3) The first-order irreversible chemical reaction is occurred on catalyst particles surface. (4) The mass transfer resistance in gas phase can be neglected. (5) The volume of liquid can be regarded as unchanged in the process of reaction.

The figure of three-dimensional mass transfer is that a flat gas–liquid interface is distributed by a large number of spherical particles. The boundary condition and its discrete process would be very complex using a single right angle or global grid in the complex geometry of the heterogeneous medium. A composite grid is effective method [13] to solve the problem. Brillman et al. [12] presented two-dimensional models which assume no variation in the z -direction, three-dimensional models by using the rotational symmetry around the line perpendicular to the gas–liquid interface. In this model, three-direction mass transfer in continuous phase and dispersed phase were considered by using orthogonal and spherical coordinate system, respectively (see Fig. 1). The composition of the composite overlapping grids is demonstrated in Fig. 2 [12,14]. As we can see, the grid consists of a set of square grid that cover the total region and annulus grid that cover the particles and the overlap where they meet. The outer annulus grid enables a numerically smooth overlap from the diffusion field around the particle to the continuous phase diffusion field. The inner radius of the outer annulus grid and the outer radius of the inner annulus grid join precisely and constitute the phase boundary. At this phase boundary, a user-defined boundary condition is implemented, accounting for continuity of fluxes and the instantaneous equilibrium distribution of the diffusing species between both phases at the interface.

A set of unsteady three-dimensional mass balance equations, respectively for continuous phase and the dispersed phase can be written as

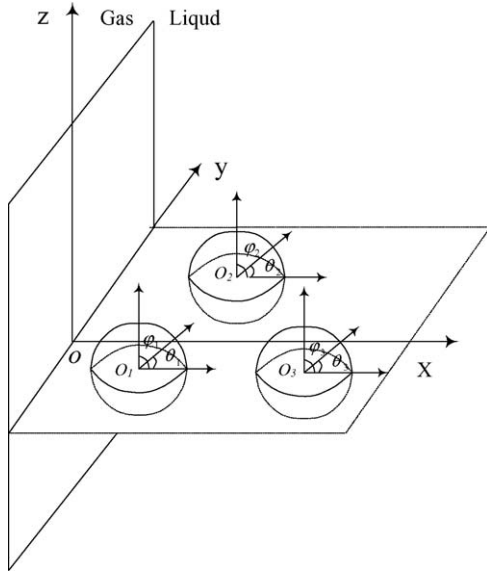


Fig. 1. Coordinate system selection of adsorptive particles distributed in liquid film zone at arbitrary.

In continuous phase (square grid)

$$\frac{\partial C_A(x, y, z, t)}{\partial t} = D_A \left(\frac{\partial^2 C_A(x, y, z, t)}{\partial x^2} + \frac{\partial^2 C_A(x, y, z, t)}{\partial y^2} + \frac{\partial^2 C_A(x, y, z, t)}{\partial z^2} \right)$$

In continuous phase around catalyst particle (outer annulus)

$$\frac{\partial C_A(r_i, \theta_i, \varphi_i, t)}{\partial t} = D_A \left[\frac{1}{r_i^2} \frac{\partial}{\partial r_i} \left(r_i^2 \frac{\partial C_A(r_i, \theta_i, \varphi_i, t)}{\partial r_i} \right) + \frac{1}{r_i^2 \sin \theta_i} \frac{\partial}{\partial \theta_i} \left(\sin \theta_i \frac{\partial C_A(r_i, \theta_i, \varphi_i, t)}{\partial \theta_i} \right) + \frac{1}{r_i^2 \sin^2 \theta_i} \frac{\partial^2 C_A(r_i, \theta_i, \varphi_i, t)}{\partial \varphi_i^2} \right]$$

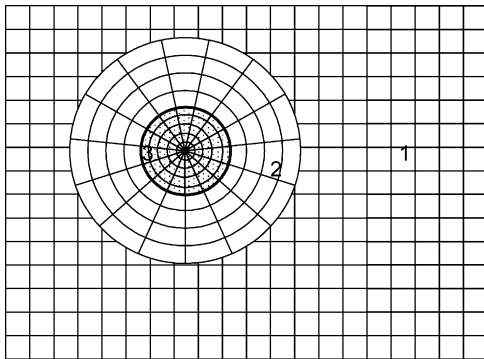


Fig. 2. Construction of the basic composite grid from component grids: (1) Rectangular grid (background), (2) annular grid (outer annulus) and (3) annular grid (inner annulus).

In catalyst particle (inner annulus)

$$\frac{\partial C_{Ad}(r_i, \theta_i, \varphi_i, t)}{\partial t} = D_{Ad} \left[\frac{1}{r_i^2} \frac{\partial}{\partial r_i} \left(r_i^2 \frac{\partial C_{Ad}(r_i, \theta_i, \varphi_i, t)}{\partial r_i} \right) + \frac{1}{r_i^2 \sin \theta_i} \frac{\partial}{\partial \theta_i} \left(\sin \theta_i \frac{\partial C_{Ad}(r_i, \theta_i, \varphi_i, t)}{\partial \theta_i} \right) + \frac{1}{r_i^2 \sin^2 \theta_i} \frac{\partial^2 C_{Ad}(r_i, \theta_i, \varphi_i, t)}{\partial \varphi_i^2} \right] - R_{Ad}$$

The first-order chemical reaction on catalyst surface

$$R_{Ad} = k_1 C_{Ad}$$

Initial and boundary conditions

$$\text{IC } t = 0, \quad x \geq 0, \quad C_A = C_b \\ r_i \geq r_{di}, \quad C_A = C_b$$

$$\text{BC } t > 0, \quad x = 0, \quad C_A = C^* = C_{A,g}/H \\ x \rightarrow \infty, \quad C_A = C_b \\ y \rightarrow \pm\infty, \quad \frac{\partial C_A}{\partial y} = 0 \\ z \rightarrow \pm\infty, \quad \frac{\partial C_A}{\partial z} = 0 \\ r_i = r_{di}, \quad D_A \frac{\partial C_A}{\partial r} = D_{Ad} \frac{\partial C_{di}}{\partial r} \\ r_i = 0, \quad \frac{\partial C_{Ad}}{\partial r} = 0$$

2.3. Numerical solution of model

The partial differential equations can only be solved numerically by using finite difference approximation. The linear six-point interpolation formula is applied for the interpolation points (i, j, k, p) on component grid [14]:

$$c_{i,j,k,p,q+1} = c_{i',j',k',p',q+1} + (ii - i')(c_{i'+1,j',k',p',q+1} - c_{i',j',k',p',q+1}) \\ - c_{i',j',k',p',q+1}(jj - j')(c_{i',j'+1,p',k',q+1} - c_{i',j',k',p',q+1}) \\ + (pp - p')(c_{i',j',k'+1,p',q+1} - c_{i',j',k',p',q+1}) \\ - c_{i',j',k',p',q+1}$$

where p' is the index of component grid from which point (i, j, k, p) the interpolated, q the index of time direction, (ii, jj, kk, p') the location of point (i, j, k, p) in component grid p' and (i', j', k', p') is the nearest grid point of (i, j, k, p) in component grid p' .

2.4. The definition of enhancement factor

According to the first Fick's law, the instantaneous flux of 'A' crossing the interface at any position is obtained from the following equation

$$N_A(y, z, t) = -D_{AB} \frac{dC_A(x, y, z, t)}{dx} \Big|_{x=0} \quad (2)$$

According to penetration theory the mass transfer flux of 'A' without the present of a dispersed phase can be written as

$$N_A^0(y, z, t) = \sqrt{\frac{D_{AB}}{\pi t}} (C_A^* - C_{A,b}) \quad (3)$$

The local instantaneous enhancement factor is defined by the ratio of these fluxes to their equivalent for gas absorption under identical conditions without the present of a dispersed phase:

$$E(y, z, t) = \frac{N_A(y, z, t)}{N_A^0(y, z, t)} \quad (4)$$

But the local enhancement factors mentioned refer always to the contact time-averaged enhancement factor

$$E(y, z) = \frac{\int_0^{\tau_c} (-D_{AB} dC_A(x, y, z, t)/dx|_{x=0}) dt}{2\sqrt{D_{AB}/\pi\tau_c}(C_A^* - C_{A,b})} \quad (5)$$

The macroscopic mass transfer enhancement factor by adding dispersed phase is defined as

$$E = \int_S E(y, z) \quad (6)$$

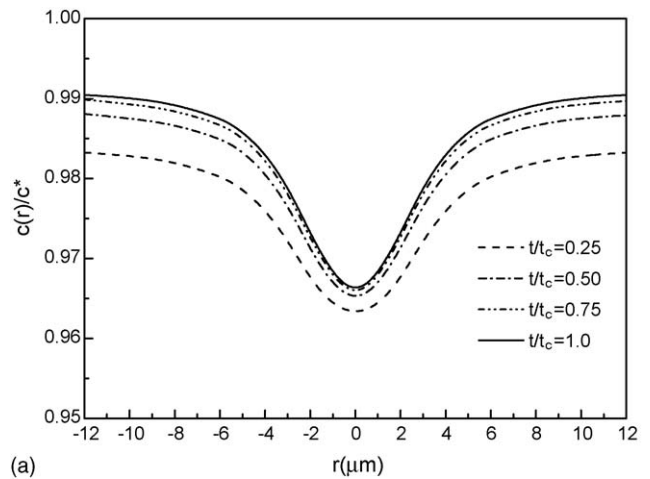
3. Results and discussion

The influence of several process parameters was taken into account by single catalyst particle simulation, particle–particle interaction was considered by two particles simulation, the macroscopic enhancement factor was predicted in catalytic slurry system by the crystal structure assumed simulation. Table 1 lists the values for the input parameters that were used for this study, which were set according to isobutene hydration to tertiary butyl alcohol catalyzed by cation exchange resin.

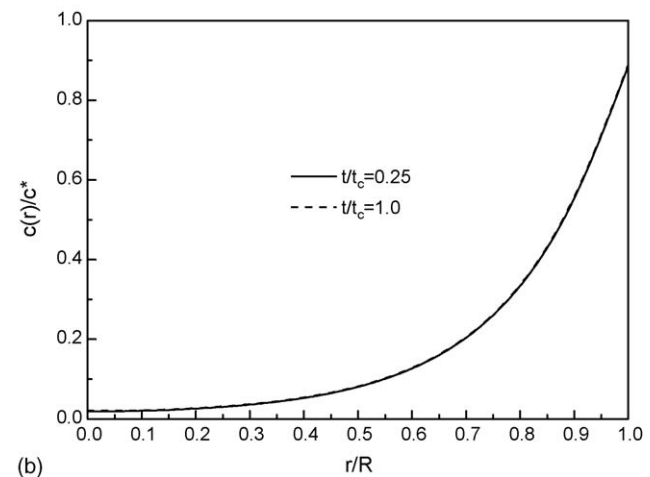
3.1. The results of simulation with one catalyst particle

The concentration profile by model simulation with single particle is given in Figs. 3 and 4, respectively. Fig. 3(a) indicates the concentration profile in y - z plane at the distance of $0.333 \mu\text{m}$ to gas–liquid interface. Fig. 3 shows that the enhancement is not only to the projection of particle to gas–liquid interface but also to ambient region.

Fig. 4(a) shows clearly that the enhancement factors obtained increase strongly with decreasing distance of the particle to the gas–liquid interface. When the ratio of the distance to particle diameter is to 1.5 the enhancement factor is little. The different of these results in Fig. 4(d) and (e) may be expressed that the influence of distance of particle to gas–liquid interface to mass transfer is more prominent than particle diameter. The effect of



(a)



(b)

Fig. 3. The concentration profile of transferred component ($k_1 = 1000 \text{ s}^{-1}$, $d_p = 4.0 \mu\text{m}$, $L = 1.0 \mu\text{m}$), (a) in liquid phase and (b) inner of catalyst particle.

the parameters, such as the distance of particles to gas–liquid interface L , particle size d_p , different contact times of liquid element τ on gas absorption rate was published by papers [11,12]. The similar results were demonstrated.

3.2. The results of simulation with two catalyst particle

The presence of other particles in the vicinity of the particle considered may affect its influence on the gas absorption. To study particle–particle interaction the simulation results of two particles in liquid film are given in Fig. 5. Fig. 5(b) shows that the influence of one particle to another is not additive relation of two single particles in the similar position. Fig. 5(a) shows that the particle–particle interaction can be neglected when the distance of two particles is $6 \mu\text{m}$.

3.3. The macroscopic enhancement factor

For calculating the macroscopic enhancement factor in catalytic slurry reactor using a heterogeneous model the distribution of catalyst particles at gas–liquid interface must be taken into account. To simply calculation, the distribution of particles in

Table 1
The parameters used in this study

D_A	$3.246 \times 10^{-9} \text{ m}^2/\text{s}$
τ_c	0.353 s
d_p	1.0, 2.0, 4.0, 8.0 μm
D_{Ad}	$2.045 \times 10^{-9} \text{ m}^2/\text{s}$
δ	30.0 μm
k_1	100, 500, 1000, 2000 s^{-1}

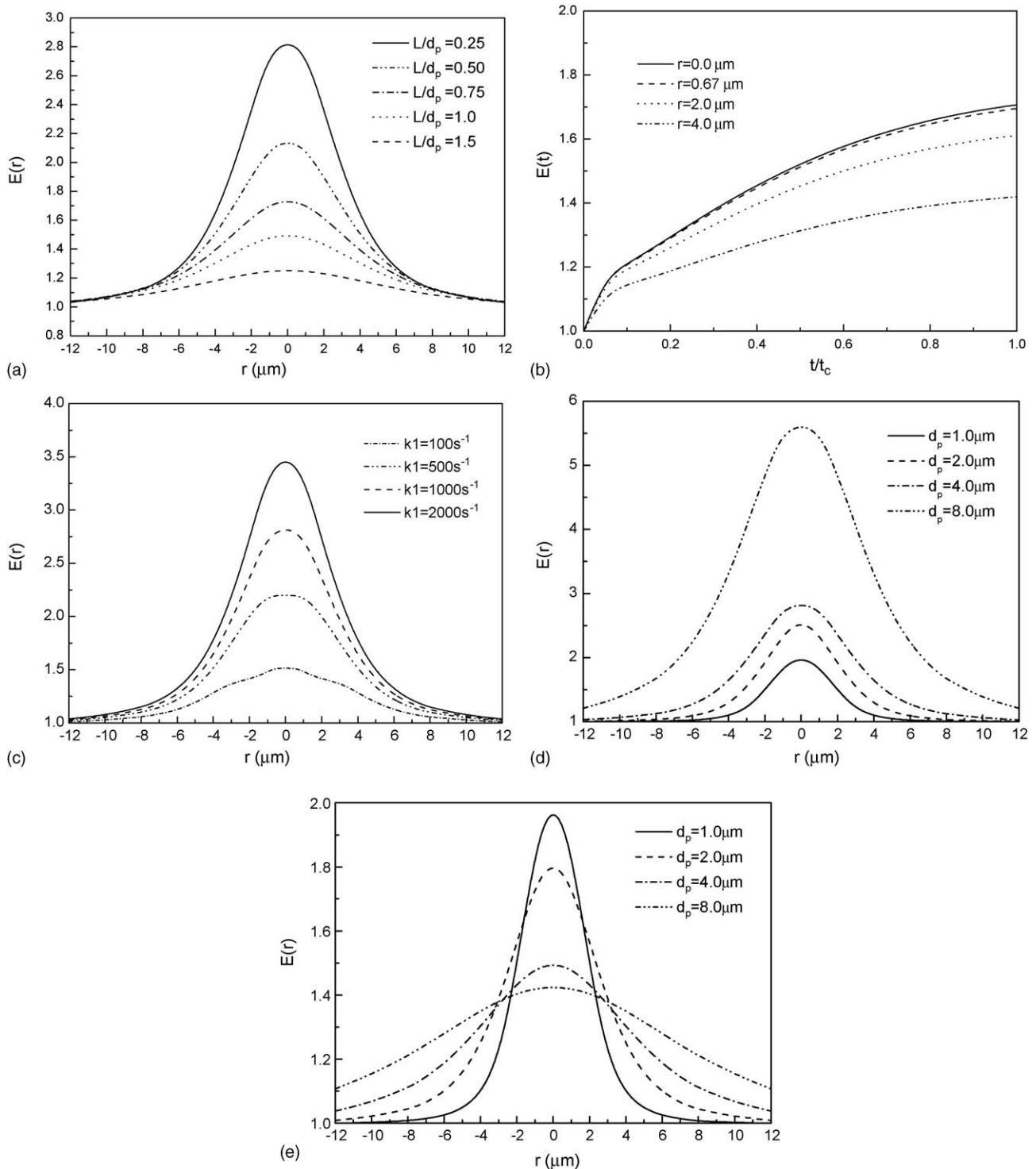


Fig. 4. The influence of several parameters to local enhancement factors by single particle simulation. (a) Effect of distance of particle to gas–liquid interface ($k_1 = 1000 \text{ s}^{-1}$, $d_p = 4.0 \mu\text{m}$); (b) the local instantaneous enhancement factor $E(t)$ at different residence time ($k_1 = 1000 \text{ s}^{-1}$, $d_p = 4.0 \mu\text{m}$, $L/d_p = 1.0$); (c) $E(r)$ at different 1th reaction rate constant ($d_p = 4.0 \mu\text{m}$, $L/d_p = 0.25$); (d) variation of particle diameter in same distance ($k_1 = 1000 \text{ s}^{-1}$, $L = 0.5 \mu\text{m}$); (e) variation of particle diameter in various distance ($k_1 = 1000 \text{ s}^{-1}$, $L/d_p = 1.0$).

the boundary layer can also be assumed to be similar to that in the bulk continuous phase and it is regular with respect to spacing and arrangement, such as a kind of crystal structure [11]. The crystal structure is selected to a investigative zone and the central zone including a particle is selected to a integral zone.

The results of the heterogeneous models by Holstvoogd et al. [15], Karve and Juvekar [7] and the one-dimensional models of Nagy [10] and Brilman et al. [16] have shown that enhancement of gas–liquid mass transfer is dominated by the first particles near the gas–liquid interface. So the first row particles are taken

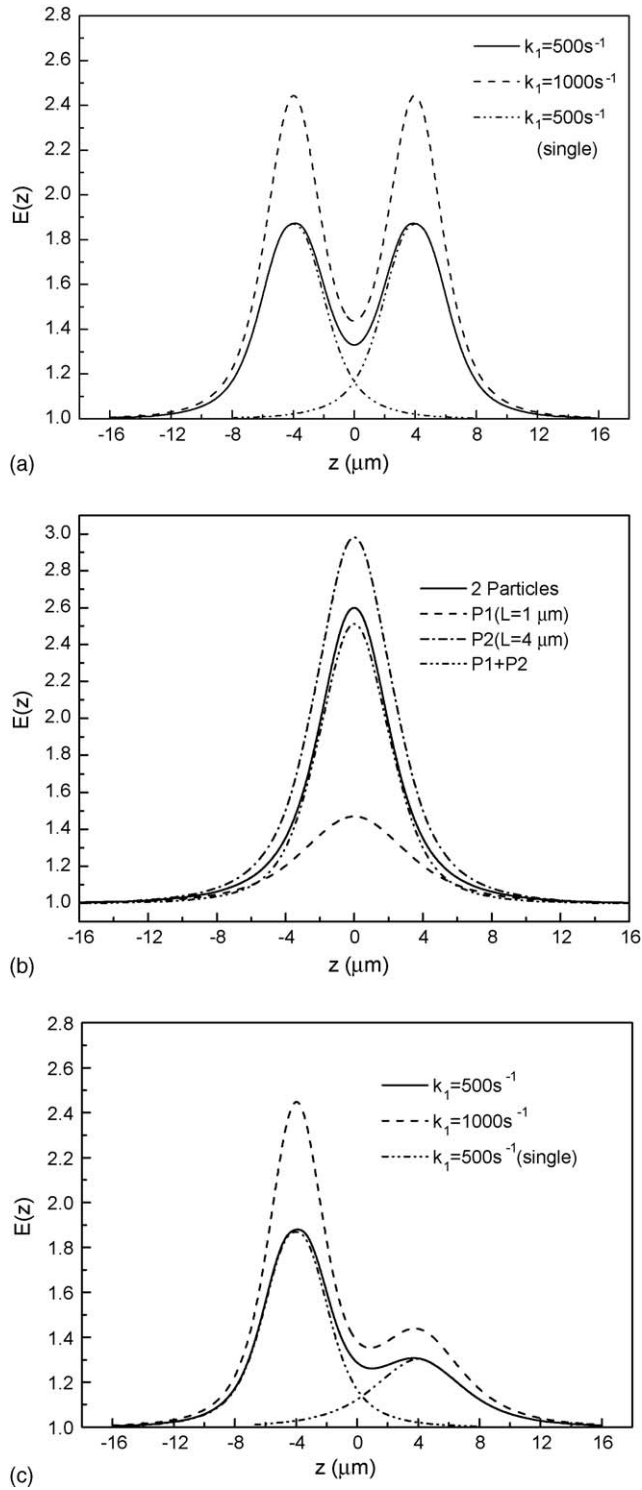


Fig. 5. The local enhancement factor with two particles in different position in liquid film: (a) $L_1=L_2=1\ \mu\text{m}$, $d_p=2\ \mu\text{m}$; (b) $L_1=1\ \mu\text{m}$, $L_2=4\ \mu\text{m}$, $d_p=2\ \mu\text{m}$, $k_1=500\ \text{s}^{-1}$; (c) $L_1=1\ \mu\text{m}$, $L_2=3\ \mu\text{m}$, $d_p=2\ \mu\text{m}$.

into account to calculate macroscopic enhancement factor in this work. Fig. 6 shows the selection of integral and investigative zone with monolayer arrays of catalyst particles in the liquid-film near the gas–liquid interface. The distance L of first droplets from the gas–liquid interface is related to the local dispersed phase holdup ϵ_s in the boundary layer [11,17]. It can be repre-

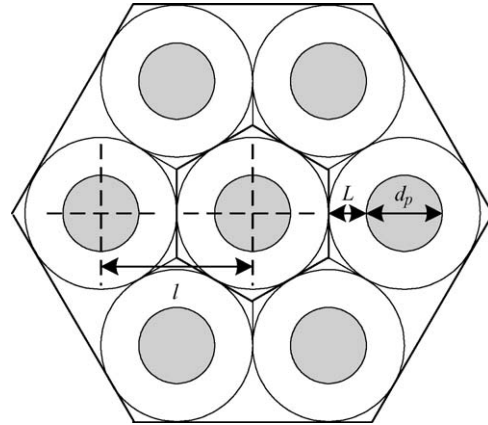


Fig. 6. The selection of integral and investigative zone with monolayer arrays of catalyst particles in the liquid-film near the gas–liquid interface.

sented by $L=(l-d_p)/2$. The distance l of two particles can be represented by $l=d_p/\sqrt[3]{\epsilon_s}$. The macroscopic enhancement in different solid particle volume content is given in Fig. 7.

The apparent viscosity of slurry and pure liquid viscosity is different due to the present of catalyst particles. The viscosity is one of the parameters that influence gas–liquid mass transfer. For calculating the macroscopic enhancement factor by adding dispersed particles the influence of apparent viscosity should be considered. According to Stokes–Einstein relationship, the relation of liquid viscosity and diffusion coefficient can be represented by

$$\frac{D_A \mu}{T} = \text{Constant} \tag{7}$$

In same temperature the diffusion coefficient is from D_0 to D_{sus} and the apparent viscosity of slurry is from μ_L to μ_{sus} after adding particles. Their relationship is

$$\frac{D_{\text{sus}}}{D_0} = \frac{\mu_0}{\mu_{\text{sus}}} \tag{8}$$

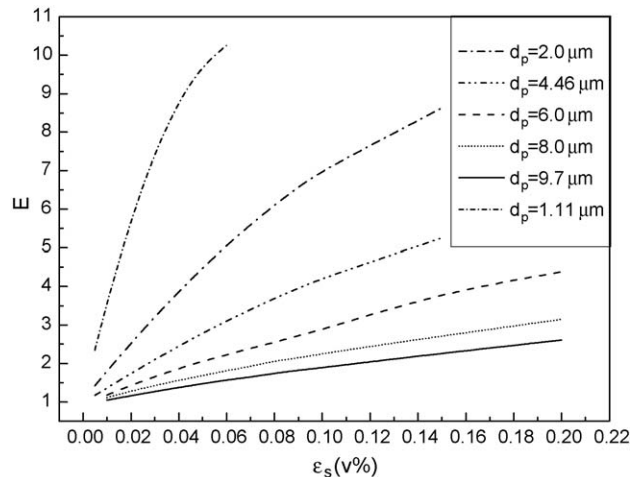


Fig. 7. Influence of solid content of particles on enhancement factor.

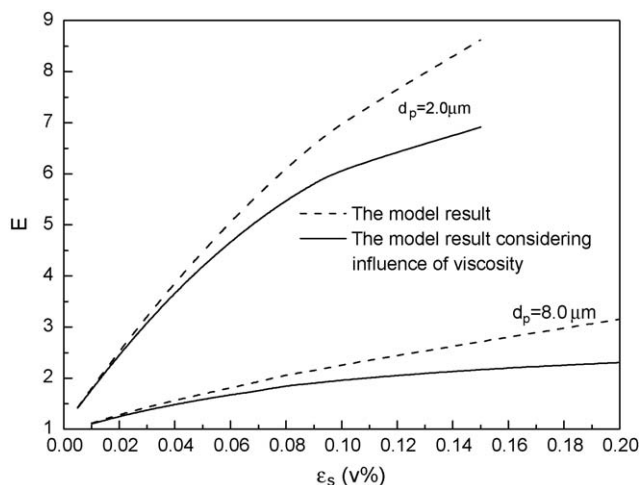


Fig. 8. Influence of viscosity on enhancement factors.

According to penetration theory the equation is obtained in same residence time

$$\frac{k_{L,sus}}{k_L} = \sqrt{\frac{\mu_0}{\mu_{sus}}} \quad (9)$$

Therefore, the correction factor of enhancement can be written as: $\sqrt{\mu_0/\mu_{sus}}$.

According to Nicodemo et al. [18] the apparent viscosity of slurry could be correlated with Eq. (10)

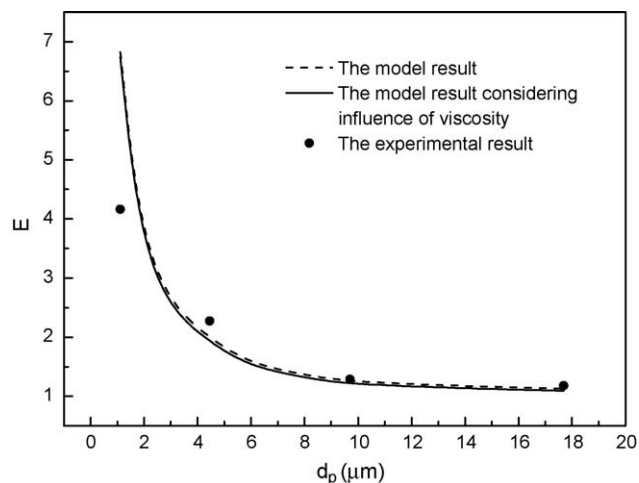
$$\frac{\mu_{sus}}{\mu_L} = \left(1 + \frac{1.25\varepsilon_v}{1 - \varepsilon_v/\varepsilon_m}\right)^2, \quad \varepsilon_m = 0.62 \quad (10)$$

Fig. 8 shows the influence of apparent viscosity to enhancement factor. As seen from Fig. 8, the enhancement effect is weakened with the increasing of the slurry apparent viscosity due to the presence of catalyst particle in liquid.

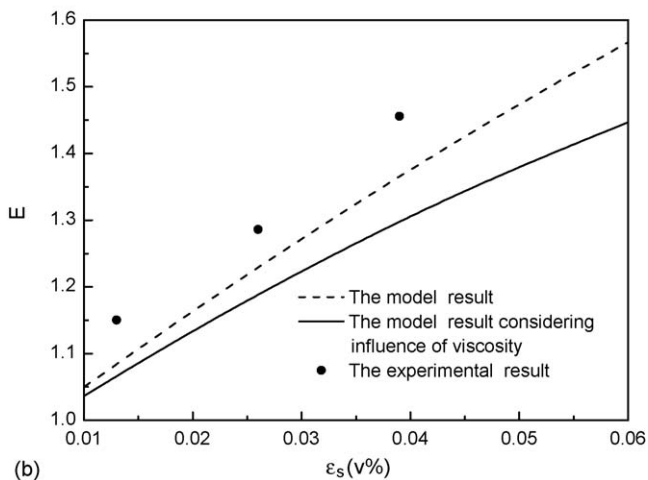
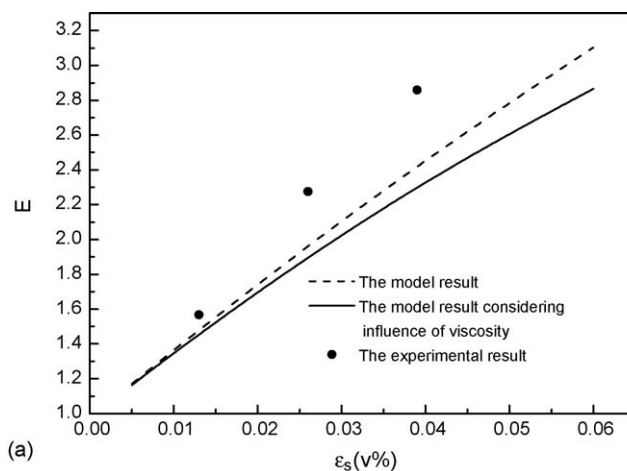
3.4. Comparison of the calculated results with experimental data

It is interesting to test the model on its capability to describe our experimental data that is for the enhancement of isobutylene mass transfer into water by fine catalyst particles [19]. The hydration of isobutylene catalyzed by acidic in homogeneous system has been shown to be first-order with respect to the isobutylene concentration. Although the macrokinetics equation of hydration of isobutylene catalyzed by cation exchange resin was obtained commonly, the kinetics of hydration of isobutylene in the internal surface of catalyst is close to intrinsic kinetics. Therefore, the first-order reaction rate constant that refer to the value in homogeneous catalytic reaction is setting to 480 s^{-1} [20]. Comparisons of model calculations with experimental data are given in Figs. 9 and 10.

The comparison of the calculated results with experimental data shows that the enhancement factor predicted by this unsteady-state three-dimensional is similar to the experimental observation. As seen from Fig. 10, the experimental data

Fig. 9. The enhancement factors of isobutene mass transfer into water in various catalyst particles diameter when the volumetric solid content is $0.026 \text{ m}^3/\text{m}^3$.

is greater than that for model predicted, the reason is that the catalyst particles diameter in experimental is volumetric average diameter and the small diameter particles is more than the bigger in quantity.

Fig. 10. The enhancement factors of isobutene mass transfer into water in various volumetric solid content: (a) $d_p = 4.46 \text{ μm}$ and (b) $d_p = 9.7 \text{ μm}$.

4. Conclusions

Unsteady-state heterogeneous mass transfer models have been developed to study the effect of fine catalyst particles near gas–liquid interface on the sparingly gas mass transfer in catalytic slurry system. Using the developed model, the particle position parameter is more importance than particle diameter from single particle simulations, the presence of other particles in the vicinity of the particle considered may affect its influence on the gas absorption, and the influence is not additive relation of two single particle in the similar position from two particles simulation. Taking all particles into account the investigated and integral region was chosen arbitrarily. The apparent viscosity of slurry has more influence on enhancement factor in higher solid content than in low solid content. The model calculation results described reasonably well the experimental data.

References

- [1] K.C. Ruthiya, J. van der Schaaf, B.F.M. Kuster, et al., Modeling the effect of particle-to-bubble adhesion in mass transport and reaction rate in a stirred slurry reactor: influence of catalyst support, *Chem. Eng. Sci.* 59 (2004) 5551–5558.
- [2] O. Ozkan, A. Calimli, R. Berber, et al., Effect of inert solid particles at low concentrations on gas–liquid mass transfer in mechanically agitated reactors, *Chem. Eng. Sci.* 55 (2000) 2737–2740.
- [3] A.A.C.M. Beenackers, W.P.M. Van Swaaij, Mass transfer in gas–liquid slurry reactors, *Chem. Eng. Sci.* 48 (18) (1993) 3109–3139.
- [4] E. Alper, W.D. Deckwer, Comments on gas absorption with catalytic reaction, *Chem. Eng. Sci.* 36 (1981) 1097–1099.
- [5] K.C. Ruthiya, J. van der Schaaf, B.F.M. Kuster, et al., Mechanisms of physical and reaction enhancement of mass transfer in a gas inducing stirred slurry reactor, *Chem. Eng. J.* 96 (2003) 55–69.
- [6] R.D. Holstvoogd, K.J. Ptasinski, W.P.M. van Swaaij, Penetration model for gas absorption with reaction in a slurry containing fine insoluble particles, *Chem. Eng. Sci.* 41 (4) (1986) 867–873.
- [7] S. Karve, V.A. Juvekar, Gas absorption into slurries containing fine catalyst particles, *Chem. Eng. Sci.* 45 (1990) 587–594.
- [8] E. Nagy, A. Moser, Three-phase mass transfer: Improved pseudo-homogeneous model, *AIChE J.* 41 (1) (1995) 23–34.
- [9] B.H. Junker, D.I.C. Wang, A.H. Hatton, Oxygen transfer enhancement in aqueous/perfluorocarbon fermentation systems: II. Theoretical analysis, *Biotechnol. Bioeng.* 35 (1990) 586–597.
- [10] E. Nagy, Three-phase mass transfer: one dimensional heterogeneous model, *Chem. Eng. Sci.* 50 (1995) 827–836.
- [11] C. Lin, M. Zhou, C.J. Xu, Axisymmetrical two-dimensional heterogeneous mass transfer model for the absorption of gas into liquid–liquid dispersions, *Chem. Eng. Sci.* 54 (1999) 389–399.
- [12] D.W.F. Brillman, M.J.V. Goldschmidt, G.F. Versteeg, et al., Heterogeneous mass transfer models for gas absorption in multiphase systems, *Chem. Eng. Sci.* 55 (2000) 2793–2812.
- [13] G. Chesshire, W.D. Henshaw, Composite overlapping meshes for the solution of partial differential equations, *J. Comput. Phys.* 90 (1990) 1–64.
- [14] W.F. Cai, Study on enhancement of gas–liquid mass transfer by fine particles in slurry system, Ph.D. Thesis, Tianjin University, Tianjin, China, 2003.
- [15] R.D. Holstvoogd, W.P.M. van Swaaij, L.L. van Dierendonck, The adsorption of gases in aqueous activated carbon slurries enhanced by adsorbing or catalytic particles, *Chem. Eng. Sci.* 43 (8) (1988) 2181–2187.
- [16] D.W.F. Brillman, W.P.M. van Swaaij, G.F. Versteeg, A one-dimensional stationary heterogeneous mass transfer model for gas absorption in multiphase systems, *Chem. Eng. Process.* 37 (6) (1998) 471–488.
- [17] C.J. Van Ede, R. van Houten, A.A.C.M. Beenackers, Enhancement of gas to water mass transfer rates by a dispersed organic phase, *Chem. Eng. Sci.* 50 (1995) 2911–2922.
- [18] L. Nicodemo, L. Nicolais, R.F. Landel, Shear rate dependent viscosity of suspensions in newtonian and non-newtonian liquids, *Chem. Eng. Sci.* 29 (3) (1974) 729–735.
- [19] J.M. Zhang, Study on enhancement of gas–liquid mass transfer by catalyst particles in slurry system, Ph.D. Thesis, Tianjin University, Tianjin, China, 2006.
- [20] J.K. Gehlawat, M.M. Sharma, Absorption of isobutylene in aqueous solution of sulphuric acid, *Chem. Eng. Sci.* 23 (1968) 1173–1180.